Technical Paper
Int'l J. of Aeronautical & Space Sci. 12(1), 63–68 (2011)
DOI:10.5139/IJASS.2011.12.1.63

IJASS
International Journal of Aeronautical and Space Science

Unsteady Subsonic Aerodynamic Characteristics of Wing in Fold Motion

Yoo-Yeon Jung*

School of Mechanical and Aerospace Engineering, Seoul National University, Seoul 151-742, Korea

Ji-Hwan Kim**

Institute of Advanced Aerospace Technology, School of Mechanical and Aerospace Engineering, Seoul National University, Seoul 151-742, Korea

Abstract

Aerodynamic characteristics of a wing during fold motion were investigated in order to understand how variations or changes in such characteristics increase aircraft performance. Numerical simulations were conducted, and the results were obtained using the unsteady vortex lattice method to estimate the lift, drag and the moment coefficient in subsonic flow during fold motion. Parameters such as the fold angle and the fold angular velocity were summarized in detail. Generally, the lift and pitching moment coefficients decreased as the angle increased. In contrast, the coefficients increased as the angular velocity increased.

Key words: Folding wing, Fold motion, Fold angular velocity

1. Introduction

Shape morphing is defined as changing the configuration of a wing in order to control the aerodynamic characteristics so that the wing may comply with the aircraft's mission profile. The morphing wing has been investigated by several groups such as the Active Aeroelastic Wing Program of NASA and the Morphing Aircraft Structures Program (MAS) provided by Defense Advanced Research Projects Agency (DARPA). Smart materials have also been researched in conjunction with the morphing wing investigations.

According to the research conducted by Rodriguez (2007), four approaches for morphing wing technology may improve aircraft performance: expand the wing's flight envelope, replace conventional control surfaces for flight control for performance and stealth advancement, reduce drag to improve range and reduce vibration, or control flutter. The benefits and future concepts of a fully morphing aircraft configuration have been investigated (Moorhouse et al., 2006). Furthermore, several concepts that focus on morphing skins were studied, such as corrugated structures, segmented structures, reinforced elastomers or flexible matrix composite tubes embedded in a low modulus membrane (Thill et al., 2008). In addition, wind tunnel tests were performed testing the morphing wing. Unsteady pressure signals were recorded and visualized in real time while the wing was being deformed to reproduce various airfoil shapes with controlling the two actuators displacements (Popov et al., 2010a, b).

In Sofla et al. (2010), morphing wing concepts were classified into three groups: planform alternation, airfoil adjustment and out-of-plane transformation. With planform alternation, wing area manipulation techniques are employed through which the wing's span and chord length are resized. Alternatively, airfoil adjustment entails designing and changing the wing profile. Out-of-plane transformation consists of altering the chordwise and spanwise camber. The folding wing is capable of adjusting the flight performance from a cruise configuration to a high speed dash configuration. During the intermediate changing configuration, aerodynamic characteristics varied

Received 23 November, 2010, Revised 16 February, 2011, Accepted 21 February, 2011
* Studesnt Researcher
** Professor, Corresponding author
E-mail: jwhkim@snu.ac.kr Tel: +82-2-880-7383 Fax: +82-2-887-2662

http://ijass.org pISSN: 2093-274x eISSN: 2093-2480

dramatically and quickly.

Finite element modeling, aerodynamic loading, and a continuous-time multi-body simulation were used to simulate the aeroelasticity of the wing of an unmanned combat aerial vehicle (Scarlett et al., 2006; Snyder et al., 2009). A methodology for the model and an analytical solution were developed in order to produce flutter solutions for a continuous representation of a two-segment uniform folding wing (Liska and Dowell, 2009). Moreover, a flutter analysis simulation was developed and tested while accounting for the nonlinearity of a wing structure (Attar et al., 2010; Tang and Dowell, 2008).

The unsteady vortex lattice method (UVLM) was developed to predict the geometry of the wake and the aerodynamic loads on the wing configuration in an incompressible flow. UVLM provides a highly effective solution of a complex problem with reasonable computational efficiency. The side-edge suction force for isolated or interaction planform was computed by applying the method (Lamar et al., 1975). Also it was applied to aircraft engine designs to improve the overall performance of both military and civil aircraft. UVLM was coupled with a typical section cascade structural model to form a set of aeroelastic equations of motion (Thake, 2009).

Most studies concerning the folding wing were performed under the assumption that the fold angle remained constant. However, this assumption produces varying results for a wing that is in motion. Accounting for this motion is a necessary action when designing the folding wing structure. In this paper, an aerodynamic analysis of a wing in the motion was performed by using UVLM.

2. Formulations

2.1 Folding wing

Figure 1 shows the schematic configuration of a wing at an instant of folding motion.

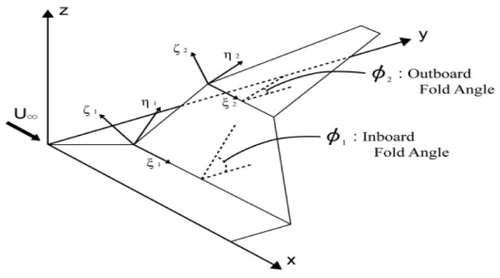

Fig. 1. Schematic configuration of the wing in fold motion.

In the figure, both $\varnothing_1$ and $\varnothing_2$ may be simultaneously varied during flight for efficient flight performance. These parameters affect aerodynamic characteristics such as lift and drag. The relationships between the global coordinates and local coordinates of each wing component are expressed as

$$\begin{Bmatrix} x \\ y \\ z \end{Bmatrix}_{inboard} = \begin{Bmatrix} \xi_1 + L_1 \tan\Lambda \\ L_1 + \eta_1 \cos\phi_1 \\ \eta_1 \sin\phi_1 \end{Bmatrix}$$
$$\begin{Bmatrix} x \\ y \\ z \end{Bmatrix}_{outboard} = \begin{Bmatrix} \xi_2 + (L_1 + L_2)\tan\Lambda \\ L_1 + L_2\cos\phi_1 + \eta_2\cos\phi_2 \\ L_2\sin\phi_1 + \eta_2\sin\phi_2 \end{Bmatrix} \quad (1)$$

where L_1, L_2 are the span length of the inboard and the outboard component, respectively, and Λ is the sweptback angle.

2.2 Unsteady vortex lattice method

The fluid surrounding the body was assumed to be inviscid, irrotational, and incompressible over the entire flowfield, excluding the solid boundaries and wakes of the body. According to Katz and Plotkin (2001), a velocity potential Φ(X, Y, Z) can be defined in the inertial frame; the continuity equation in this frame becomes

$$\nabla^2\Phi=0 \text{ (in X, Y, Z coordinates)} \quad (2)$$

and the first boundary condition requiring zero normal velocity across the solid boundaries is

$$(\nabla\Phi+v)\cdot n=0 \text{ (in X, Y, Z coordinates)} \quad (3)$$

where v is the velocity of the surface and n is the vector normal to the moving surfaces. Also the second boundary condition is diminishing the flow disturbance far from the body.

$$\lim_{|R-R_0|\to\infty} \nabla\Phi = 0 \quad (4)$$

where R=(X, Y, Z).

For unsteady flow, the Kelvin conditions supply an additional equation in determining the streamwise strength of the vorticity shed into the wake. In general, the condition states that in the potential flow region the angular momentum cannot change, and thus the circulation Γ around a fluid curve enclosing the wing and its wake is conserved:

$$\frac{d\Gamma}{dt} = 0 \quad \text{(For any t)} \quad (5)$$

DOI:10.5139/IJASS.2011.12.1.63

From the continuity equation, the general solution can be obtained by integrating the contribution of the basic solution of source σ and doublet μ distributions over the surface and wakes of the body,

$$\Phi(x,y,z) = \frac{1}{4\pi}\int_{body+wake} \mu n \cdot \nabla\left(\frac{1}{r}\right) dS - \frac{1}{4\pi}\int_{body} \sigma\left(\frac{1}{r}\right) dS \tag{6}$$

Although, this formulation does not directly include a vortex distribution, doublet distributions can be replaced by equivalent vortex distributions.

On the other hand, the wake shed from the trailing edge of the lifting surfaces can be modeled by vortex distributions. The strength of each vortex Γ_{W_i} is equal to the vorticity shed during the corresponding time step Δt such that

$$\Gamma_{W_i} = \int_{t-\Delta t}^{t} \gamma_W(t) U(t)\, dt \tag{7}$$

Consequently, the strength and location of the vortex must be specified for each vortex element. The wake vortex location should be aligned with the trailing edge and be located closer to the latest position of the trailing edge.

The zero normal velocity boundary condition on the surface (Q_{nk}=0) for an arbitrary collocation point k can be obtained the following equations.

$$Q_{nk} = a_{k1}\Gamma_1 + a_{k2}\Gamma_2 + a_{k3}\Gamma_3 + \cdots + a_{km}\Gamma_m + \left[U(t) + u_W, V(t) + v_W, W(t) + w_W\right]_k \cdot n_k = 0 \tag{8}$$

Once the computations of the influence coefficients and the right-hand side vector are completed, the zero normal flow boundary condition on all collocation points of the wing will result as

$$[A]\{\Gamma\} = \{B\} \tag{9}$$

And then the circulation can be obtained from this equation. Furthermore, the aerodynamic forces can be computed by using the Bernoulli equation and the pressure difference can be as follows.

$$\Delta p_{i,j} = \rho\left\{\left[U(t) + u_W, V(t) + v_W, W(t) + w_W\right]_{i,j} \cdot \tau_i \frac{\Gamma_{i,j} - \Gamma_{i-1,j}}{\Delta c_{i,j}} + \left[U(t) + u_W, V(t) + v_W, W(t) + w_W\right]_{i,j} \cdot \tau_j \frac{\Gamma_{i,j} - \Gamma_{i,j-1}}{\Delta b_{i,j}} + \frac{\partial}{\partial t}\Gamma_{i,j}\right\} \tag{10}$$

where $\Delta c_{i,j}$ and $\Delta b_{i,j}$ are the panel lengths in the i-th and j-th directions, respectively. Similarly, τ_i and τ_j are the panel tangential vectors in i and j directions.

Then the load of this panel is

$$\Delta F = -\left(\Delta p \Delta S\right)_{i,j} n_{i,j} \tag{11}$$

Therefore, the total forces and moments are obtained by the load of each panel. (Editor's Note: This section is very nicely written)

3. Numerical Simulation

Fold angle and angular velocity were the most important parameters in the numerical simulation. These parameters potentially change the aerodynamic characteristics of a wing while the wing is in motion. The simulation and verification were performed by C++ and MATLAB.

3.1 Model configuration

The wing consisted of three parts: the inboard and outboard components which undergo rotating motion and the body component that is not subject to motion. For this simulation, only the inboard component was assumed to rotate about the x-axis from 0° to 85°; $\varnothing_2$ was set to zero.

The location of the wake behind the trailing edge was varied according to fold angle. Thus, if the wing is in motion, the wake will follow the trailing edge, and then the effects of the wake will not be same for a constant angle. The location of the wake in motion is shown in Fig. 2.

Additionally, the collocation points of each aerodynamic panel were changed during fold motion and then the circulation in Eq. (9) will be changed. As a result, the varied circulation value of the panels will produce differing aerodynamic characteristics. Therefore, the characteristics

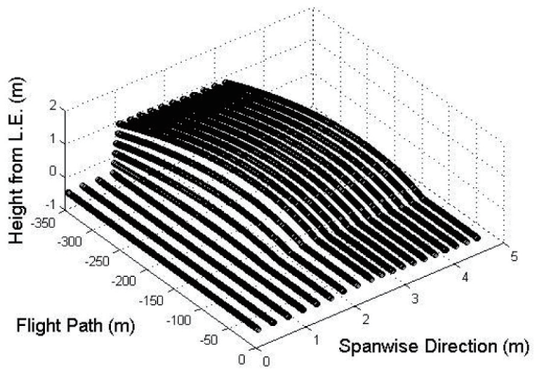

Fig. 2. The location of the wake behind the trailing edge in the motion.

Table 1. Model configuration (unit: inch)

Chord	Body	180 (root)	144 (tip)
	Inboard	144	60
	Outboard	60	21
Span	Body	36	
	Inboard	54	
	Outboard	84	
Sweepback angle		45°	

of the wing were varied for the wing in fold motion.

Table 1 represents the model details (Lee and Chen, 2006). This model is an innovative aircraft design proposed by Lockheed Martin as part of the DARPA MAS (Lee and Chen, 2006).

3.2 Verification

For the verification of this work, an aerodynamic analysis was performed using a simple uncambered, rectangular wing model that was suddenly set into a constant-speed forward flight, as given by Katz and Plotkin (2001). The results were almost equal to the data of the reference as shown in Fig. 3.

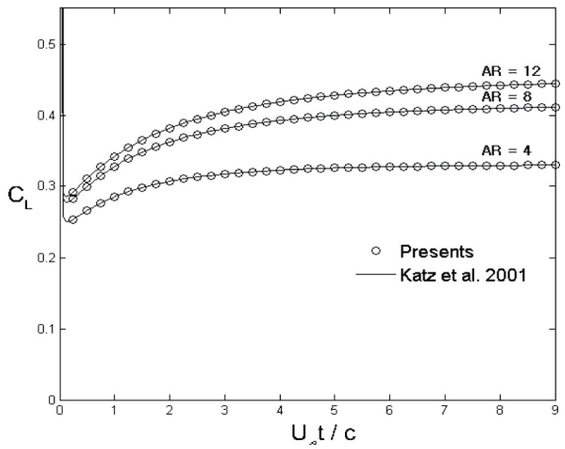

Fig. 3. Comparison of the transient lift coefficient variation for $U_\infty \Delta t/c$=1/16 and a=5°.

4. Results and Discussion

The freestream velocity was 50 m/s, the air density was assumed as 1 kg/m^3 and the angle of attack was 5°. Also, in order to reduce the effect of sudden acceleration, the folding was initiated at 2 seconds. As shown in Fig. 4, the total lift

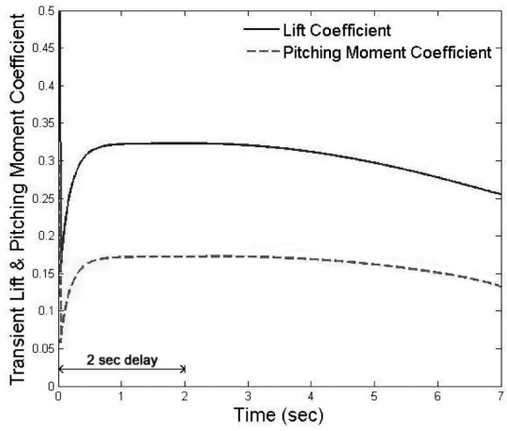

Fig. 4. Transient lift coefficient and pitching moment coefficient in fold motion.

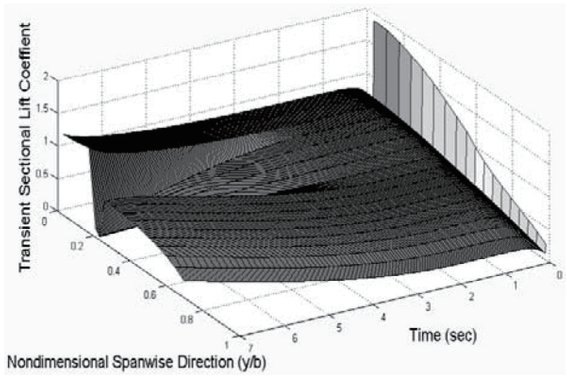

Fig. 5. Sectional lift coefficient variation in fold motion.

coefficient and pitching moment coefficient decreased.

If the aerodynamic forces orthogonally acting on the individual panels were taken into consideration, the tendency of the transient lift coefficient could be slightly different from that given in Fig. 4. But, the z-direction forces were only considered in the analysis, which was the direction of the total lift.

In Fig. 5, the sectional lift coefficient is shown. The coefficient of the inboard component largely decreased.

The distribution of the sectional lift changed as the fold angle reached 90°. As shown in Fig. 5, aerodynamic characteristics of the wing in fold motion varied. Additionally, the decrease of the lift coefficient of the inboard component was observed as the fold angle increased.

The pressure coefficient vs. nondimensional chord-wise direction of each part is represented in Fig. 6.

Large variations did not occur except for in the inboard component, similar as Fig. 5.

DOI:10.5139/IJASS.2011.12.1.63

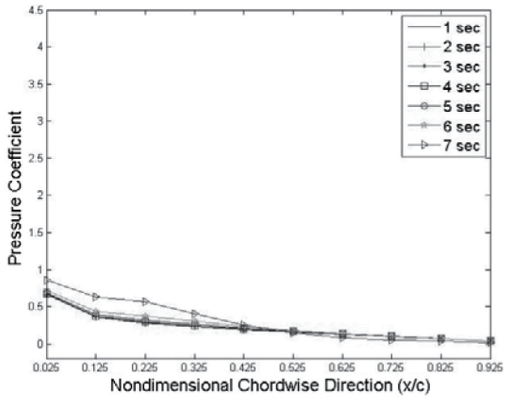

(a) Pressure coefficient at body part

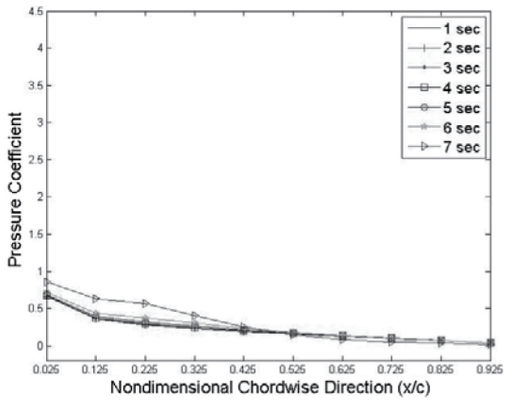

(b) Pressure coefficient at inboard part

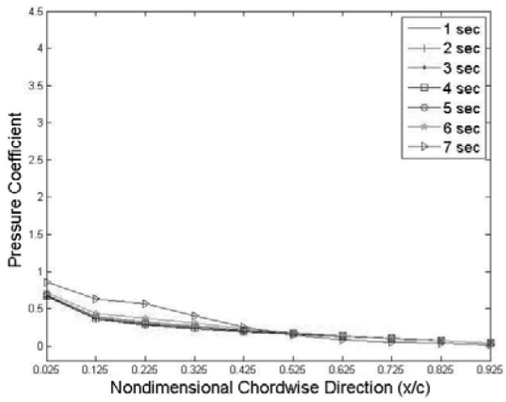

(c) Pressure coefficient at outboard part

Fig. 6. Pressure coefficient vs. nondimensional chordwise direction.

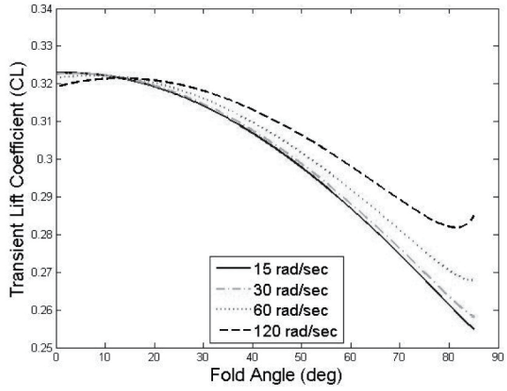

(a) Transient lift coefficient variation

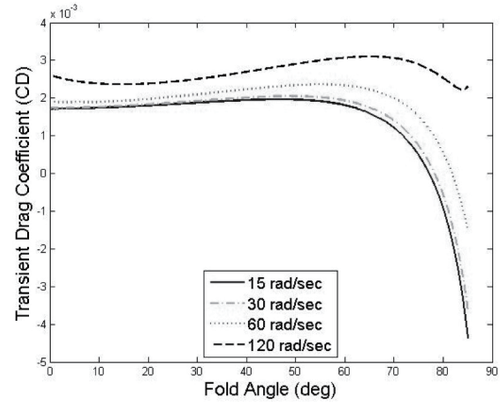

(b) Transient drag coefficient variation

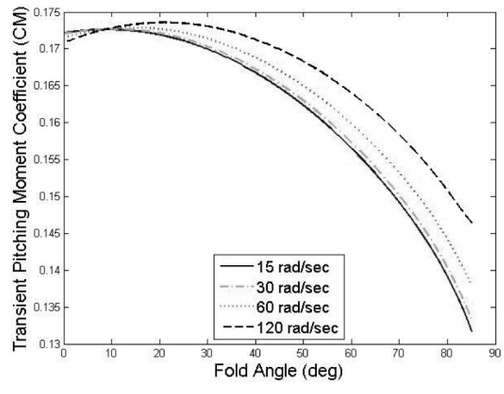

(c) Transient pitching moment coefficient variation

Fig. 7. Aerodynamic characteristics variation.

The fold angular velocity, $\dot{\phi}$ was another parameter taken into consideration. The large fold angular velocity produced opposite effects in the aerodynamic characteristics in comparison to the small angular velocity.

In Fig. 7, the variations of transient lift coefficient, drag coefficient and pitching moment coefficient are represented

for each angular velocity.

From these results, a larger angular velocity gained more lift, drag and also pitching moment. Moreover, the lift coefficient decreased and the drag coefficient increased as the fold angle increases except case of 120 rad/sec.

5. Conclusions

An aerodynamic model for a folding wing was developed and vortex lattice method was used for the analysis. The model was derived from the DARPA MAS and analyzed for various fold angles and fold angular velocities.

The location of the wake behind the trailing edge varied according to the fold angle and the fold angular velocity. Thus, aerodynamic characteristics such as lift, drag and moment of the wing in fold motion also varied during flights. Also as the fold angle increased, the lift coefficient and the drag coefficient decreased. This indicates that the folded wing configuration was more suitable to dash. However, the results of this paper showed that the effect of a large fold angular velocity was also an important factor that cannot be ignored.

According to the results obtained in this study, the various aerodynamic characteristics in fold motion affect aeroelastic characteristics. Therefore, flutter analysis of a folding wing during the motion will be investigated.

References

Attar, P. J., Tang, D., and Dowell, E. H. (2010). Nonlinear aeroelastic study for folding wing structures. *AIAA Journal*, 48, 2187-2195.

Katz, J. and Plotkin, A. (2001). *Low Speed Aerodynamics*. 2nd ed. Cambridge: Cambridge University Press. p. 430.

Lamar, J. E., Gloss, B. B., and Langley Research Center. (1975). *Subsonic Aerodynamic Characteristics of Interacting Lifting Surfaces with Separated Flow Around Sharp Edges Predicted by a Vortex-Lattice Method*. Washington, DC: National Aeronautics and Space Administration.

Lee, D. H. and Chen, P. C. (2006). Nonlinear aeroelastic studies on a folding wing configuration with free-play hinge nonlinearity. *47th AIAA/ASME/ASCE/AHS/ ASC Structures, Structural Dynamics and Materials Conference*, Newport, RI. pp. 1754-1775.

Liska, S. and Dowell, E. (2009). Continuum aeroelastic model for a folding-wing configuration. *AIAA Journal*, 47, 2350-2358.

Moorhouse, D., Sanders, B., Von Spakovsky, M., and Butt, J. (2006). Benefits and design challenges of adaptive structures for morphing aircraft. *Aeronautical Journal*, 110, 157-162.

Popov, A. V., Grigorie, L. T., Botez, R., Mamou, M., and Mebarki, Y. (2010a). Closed-loop control validation of a morphing wing using wind tunnel tests. *Journal of Aircraft*, 47, 1309-1317.

Popov, A. V., Grigorie, L. T., Botez, R., Mamou, M., and Mebarki, Y. (2010b). Real time morphing wing optimization validation using wind-tunnel tests. *Journal of Aircraft*, 47, 1346-1355.

Rodriguez, A. R. (2007). Morphing aircraft technology survey. *45th AIAA Aerospace Sciences Meeting*, Reno, NV. pp. 15064-15079.

Scarlett, J. N., Canfield, R. A., and Sanders, B. (2006). Multibody dynamic aeroelastic simulation of a folding wing aircraft. *47th AIAA/ASME/ASCE/AHS/ASC Structures, Structural Dynamics and Materials Conference*, Newport, RI. pp. 6398-6407.

Snyder, M. P., Sanders, B., Eastep, F. E., and Frank, G. J. (2009). Vibration and flutter characteristics of a folding wing. *Journal of Aircraft*, 46, 791-799.

Sofla, A. Y. N., Meguid, S. A., Tan, K. T., and Yeo, W. K. (2010). Shape morphing of aircraft wing: Status and challenges. *Materials and Design*, 31, 1284-1292.

Tang, D. and Dowell, E. H. (2008). Theoretical and experimental aeroelastic study for folding wing structures. *Journal of Aircraft*, 45, 1136-1147.

Thake, M. P., Jr. (2009). *Effect of Mistuning on Bending-Torsion Flutter Using a Compressible Time-Domain Aerodynamic Theory*. Senior Honors Thesis, The Ohio State University.

Thill, C., Etches, J., Bond, I., Potter, K., and Weaver, P. (2008). Morphing skins. *Aeronautical Journal*, 112, 117-139.

DOI:10.5139/IJASS.2011.12.1.63